INTELLIGENT SYSTEMS AND SUSTAINABLE ENERGY
E-ISSN: ### - ###
VOLUME 1, ISSUE 1, 2026, pages 38 – 46
DOI: https://doi.org/10.15282/isse.1.1.2026.14277

RESEARCH ARTICLE

Electrical capacitance tomography for detecting rice moisture content in a container

Farrina Izzati Faizal Nor[1], Mohd Mawardi Saari[1], Nurul A'in Nadzri[1], Nurhafizah Abu Talip Yusof[1,2], Ruzairi Abdul Rahim[3], Sia Yee Yu[4], Yasmin Abdul Wahab[1*]

[1]Faculty of Electrical & Electronics Engineering Technology, Universiti Malaysia Pahang Al-Sultan Abdullah, 26600 Pekan, Pahang, Malaysia
[2]Centre for Research in Advanced Fluid & Processes (Fluid Centre), Universiti Malaysia Pahang Al-Sultan Abdullah, Lebuhraya Tun Razak, 26300 Gambang, Kuantan, Pahang, Malaysia
[3]Process Tomography Research Group (Protom-i), School of Electrical Engineering, Faculty of Engineering, Universiti Teknologi Malaysia, 81310 UTM Skudai, Johor, Malaysia
[4]LOGO Solution Sdn. Bhd., Suite 0525, Level 5, Wisma SP Setia, Jalan Indah 15, Bukit Indah, 79100 Iskandar Puteri Johor Malaysia

Abstract - Rice moisture content is an important consideration in agriculture, influencing storage stability, food safety, and economic value. The feasibility of traditional measurement techniques for real-time monitoring in bulk storage is limited since they are frequently intrusive, costly, or time-consuming. In this study, a non-invasive Electrical Capacitance Tomography (ECT) device for determining the moisture content of rice in a vertical rectangular container is developed. An Arduino Nano microcontroller, a signal generator, a four-channel ECT sensor, and high-speed operational amplifiers (LT1360 and LT1364) for signal conditioning are all used in the suggested system. By monitoring changes in permittivity brought on by moisture levels, the technique enables cross-sectional mapping without coming into direct touch with the grain. The testing results show that the system can differentiate between different moisture conditions, and that the voltage values for rice with moisture are significantly higher than those for dry rice. In particular, phantom size and spatial arrangement led to different voltage swings, with some installations reaching peak levels of 8.8V. The outcomes highlight ECT's promise as a cost-effective and dependable substitute for real-time agricultural applications. Future work includes optimization of circuit performance, tomogram image reconstruction and machine learning calibration for industrial scale grain storage.

ARTICLE HISTORY
Received : 13 March 2026
Revised : 20 April 2026
Accepted : 27 April 2026
Published : 30 April 2026

KEYWORDS
Electrical capacitance tomography
Rice moisture content
Non-invasive measurement
Agriculture
Sensor system

1. Introduction

Rice is the main food supply for billions of people throughout the world. The moisture content during storage and processing greatly affects the quality of rice. While less moisture increases grain breakage during milling and decreases economic value, excess moisture encourages mold growth and contamination. The available moisture measurement techniques are not suitable for monitoring in agricultural applications as they are either intrusive, sluggish, non-portable and costly. Electrical Capacitance Tomography (ECT) is a non-invasive approach to identify dielectric changes related to moisture content. ECT permits monitoring without direct contact with the rice and delivers cross sectional data, unlike point probes. This strategy is certainly useful in bulk storage systems where changes in moisture can affect the overall quality of rice. This project is focused on the design and development of a four-channel ECT sensor jig for the detection of moisture in rice in vertical containers, implementing electronic measurement circuits like signal generators and signal conditioning and assessing the performance of the sensor for the differentiation of moisture conditions. The proposed system aims to illustrate the potential of ECT for agricultural applications by offering a reliable and cost-effective means of monitoring rice moisture.

1.1. ECT Current Research

Rice moisture content monitoring is necessary for food safety, increasing milling yield and storage stability. Studies have shown that moisture levels above 14% will enhance the occurrence of mold and aflatoxin contamination [1], whereas moisture levels below 12% will increase the breakage of grain during milling [2]. Traditional methods like oven drying (AOAC Standard 934.01) are accurate but time consuming and invasive, and thus impractical for large scale or real time monitoring [3]. Few alternatives in sensor technology have been explored. Capacitive and radiofrequency handheld probes are simple and portable for measurements, however they are limited to specific regions and often ignore spatial differences in bulk materials [2]. Then, near-infrared (NIR) spectroscopy provides accurate surface moisture detection but is expensive and sensitive to sample texture [4]. However, microwave resonance techniques are less suitable for normal agricultural use since they need a difficult calibration even if they can profile moisture internally [5], [6]. These drawbacks point to the need for advanced, portable, non-invasive and affordable techniques.

***CORRESPONDING AUTHOR | Yasmin Abdul Wahab** | ✉ yasmin@umpsa.edu.my

Electrical Capacitance Tomography (ECT) is a promising technique for this problem. ECT is a technique that allows the cross-sectional and volumetric mapping by detecting permittivity variations due to moisture differences without the necessity of destructive sample [7]. Research has demonstrated its usefulness in monitoring soil moisture [8], coffee bean drying [9], and grain storage [10]. Recent advances, such as multi-electrode arrays and machine-learning calibration, have enhanced the accuracy to within ±2% compared to X-ray CT [11], [12]. These findings indicate the reliability of ECT as an approach for moisture measurement in the field of agriculture and ECT is a good tool for the assessment of the moisture content of rice during storage.

1.2. Basic Principle of ECT

Electrical Capacitance Tomography (ECT) is an imaging approach capable of imaging the permittivity distribution inside a material without damaging the material [13], [14]. ECT is widely employed in many applications such as industrial process control, multiphase flow monitoring, and detection of soil moisture content in agriculture. The electrodes are arranged around a preset area and the capacitance between pairs of electrodes is measured, the variations in permittivity are utilized to reconstruct the image. The basic principle of ECT connects on the relationship between capacitance (C), voltage (V), and charge (Q), described by the following equation:

$$C = \frac{Q}{V} \quad (1)$$

This formula demonstrates the direct correlation between capacitance and the amount of charge stored per unit voltage. In actual ECT systems, a transmitting electrode is subjected to voltage stimulation, and the potential changes that arise are measured by the receiving electrodes. These voltage readings indicate changes in the electric field, which are dependent on the dielectric material's permittivity between the electrodes.

Voltage signals are more frequently quantified in real-time systems than raw capacitance because they are easier to digitize. Water's high dielectric constant (~80) in comparison to dry air or grains makes it useful for measuring moisture content since the change in measured voltage indirectly signals a change in capacitance due to material permittivity changes [15]. As a result, the presence of moisture causes notable changes in permittivity, which in turn modifies the voltage response of the system. ECT image reconstruction is led by Poisson's equation [16], [17], [18], [19], [20], a basic equation in electrostatics, where Φ is the electrical potential, ε is the electrical permittivity of the material, ρ is the electric charge density, and ∇ is the divergence operator:

$$\nabla.(\varepsilon \nabla \Phi) = -\rho \quad (1)$$

This formula demonstrates how variations in electrical permittivity (ε) affect the electric potential distribution (Φ), which in turn influences the voltages measured between electrodes. For this reason, spatial permittivity distribution is used in ECT imaging instead of resistivity or direct conductivity. The permittivity of water is significantly higher than that of most dry materials. This makes it possible for ECT to efficiently identify the distribution of moisture. For instance, a study used ECT to demonstrate grain moisture sensing. Moisture patterns that point-based probes would overlook can be found using this method. To monitor voltage changes brought on by fluctuations in permittivity brought on by moisture during rice storage, a capacitance sensor has been created. ECT creates volumetric, cross-sectional pictures, in contrast to resistive or NIR techniques. Because of this, it's a better choice when moisture is dispersed unevenly.

2. Materials and Methods

Using a four-channel sensor configuration, the suggested Electrical Capacitance Tomography (ECT) was created to identify the moisture level of rice in a vertical container. As seen in Figure 1 below, the process consists of an ECT sensor, sensor jig design, and electronic circuit construction. The hardware system consists of a signal generator circuit, which is a function generator and demultiplexer, a vertical rectangular rice container with an ECT sensor jig, a signal conditioning circuit and an Arduino controller. The signal generator supplies the required frequency and voltage to the selected transmitter, while the demultiplexer enables transmitter switching. Signals received at the receiver channels are amplified by the signal conditioning circuit. Then, the Arduino controls channel switching and manages transmitter and receiver selection and performs analog-to-digital conversion (ADC) so the sensor data can be processed and displayed on a computer.

2.1. Project Setup

This setup in Figure 2 includes a function generator that supplies a 500 kHz frequency and 10 Vpp voltage. These signals are connected to the ECT sensor channels, which are attached to a sensor jig surrounding the rice container. This non-invasive arrangement ensures no contamination of the rice. The transmitted and received signals are then read and observed using an oscilloscope.

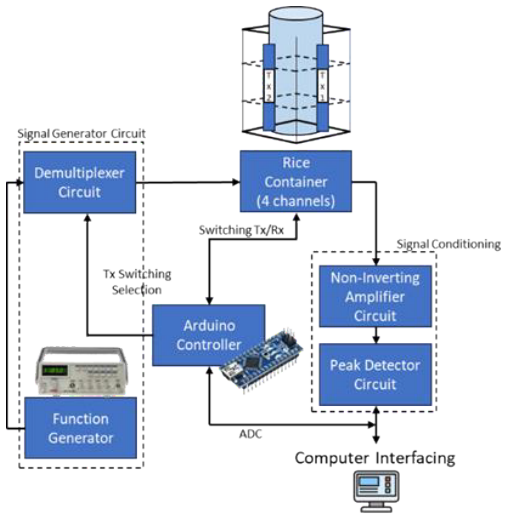

Figure 1. Basic block diagram of the project

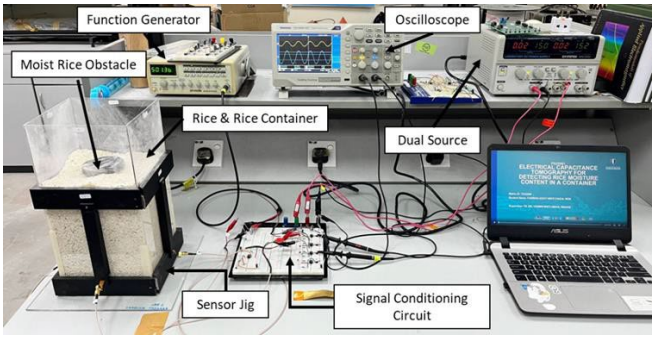

Figure 2. Project setup

2.2. ECT Sensor

The sensor used for this project is the ECT sensor. The concept of this sensor involves detecting variation in electrical permittivity distribution in a container. In this project, a rice container is used, where the contents act as a dielectric medium. The electrode array is placed around the container wall. Figure 3 shows the actual ECT sensor used in this project, whose the sensing area has dimensions of 90 mm in height and 20.57 mm in width.

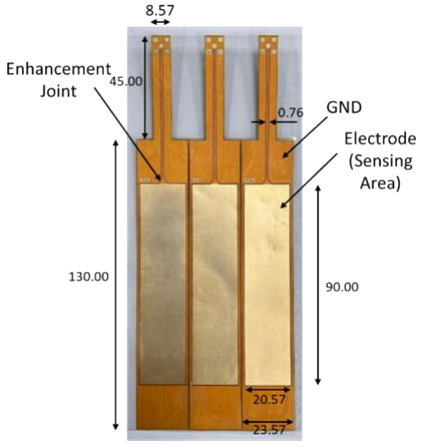

Figure 3. ECT Sensor

There were two designs proposed for this project. The initial design used a cylindrical rice container with a diameter of 75mm and a length of 200mm. The sensor jig was designed using Solidworks, as shown in Figure 4 (a). It has the same diameter as the container and includes four vertical slots to mount the ECT sensor channels around the circumference, each with a length of approximately 155mm. This project designs the hardware considering a non-invasive way. Figure 5 below illustrates the final of the first design, which includes the rice container at the center arranged vertically along with the sensor jig. However, the jigs were not practical and had imperfect printing, so the ECT vertical sensors were not able to be attached properly and probably were not really practical to make sensor readings, and reading measurements might not be accurate. So, a new square shape of rice container was proposed, and an improved design of sensor jig was created

to overcome the issues. The square geometry simplifies the jig's printed surface, ensuring a better fit against the container walls. The rice container has roughly a width of 176 mm with a length of 250 mm. The sensor jig was designed using the 3D software Solidworks. The sensor jig also has the same size as the container, wrapping around the container with 4 jigs to attach the four channels of the ECT vertical sensor around the circumference of the rice container, which the jigs each have approximately 180 mm of length for the sensor. Figure 4 (b) illustrates the final design.

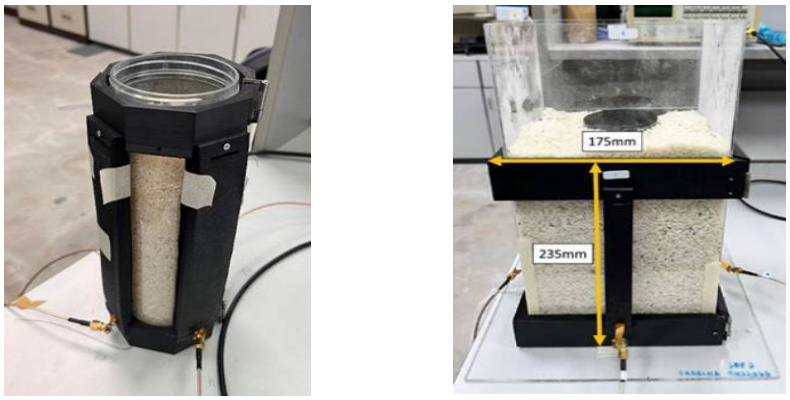

(a) (b)

Figure 4. (a) Initial design of sensor jig; (b) Final design of sensor jig

Four-channel ECT sensors are placed in a non-invasive way around the outer side of the rice container, and each channel can operate as either a transmitter (Tx) or receiver (Rx). During the experiment, one channel acts as the transmitter while the other three function as receivers. This step is repeated until all channels have been used as the excitation source. The sensors are attached to a vertical sensor that surrounds the rice container without any contact with the rice inside the container. Figure 5 shows the arrangement of the sensors, showing an example where channel 1 is the transmitter and other channels are receivers. The phantoms are cylindrical containers of several sizes (small, medium, and large) with black lids. The container was made of plastic. These phantoms were filled with moist rice to better represent moist rice regions inside the dry rice bulk. This configuration enables the system to evaluate its ability to determine moisture induced localized permittivity variation.

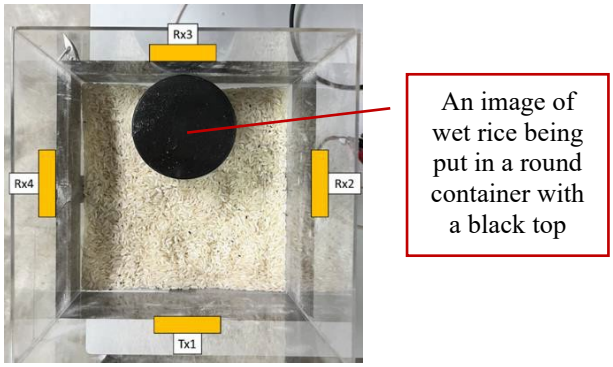

Figure 5. ECT Sensor Arrangement

2.3. Electronic Measurement Circuits

The electronic measurement technique has two main circuits, which are the signal generator circuit and the signal conditioning circuit. The signal generator circuit consists of a function generator and a demultiplexer circuit. Figure 7 shows a basic illustration of the demultiplexer that is used in the system. The demultiplexer is connected to the function generator and is responsible for selecting which channel will act as the transmitter (Tx). This setup allows any channel to be chosen automatically as the transmitter, eliminating the need for manual switching, which can be time-consuming. The selection process is controlled by programming the Arduino controller. Unfortunately, the development of an automated switching circuit for the channels was discontinued due to time constraints; consequently, the switching was performed manually.

The signal conditioning circuit consists of a non-inverting amplifier circuit and a peak detector circuit (refer to Figure 6). The non-inverting amplifier circuit, which is to amplify the signal transmitted at the receiver, is connected to the peak detector circuit to detect the peak of the voltage from the amplified signal. In this project, LT1361 is used for the non-inverting amplifier circuit because it offers fast response, low power consumption, and low distortion, making it ideal as a single high-speed operational amplifier. Meanwhile, the LT1364 is selected for the peak detector circuit for its ability to respond quickly to fast voltage changes and provide accurate peak detection. As a quad high-speed operational amplifier, the LT1364 delivers fast signal response, high accuracy, and low noise, ensuring reliable peak signal capture even during rapid voltage fluctuations. Figure 6 also shows the simulation result of the amplified signal voltage, which is 3.44 V that

is close enough to the calculated output. In Figure 6, the yellow line represents the output reading signal from the Rx (receiver), and the blue line represents the amplified signal, meanwhile the purple line represents the peak detector signal. However, when the simulated circuit was applied to the real circuit, the output from the sensor reading was not amplified, and the peak detector did not come out as expected, which should have been the straight line (see Figure 7).

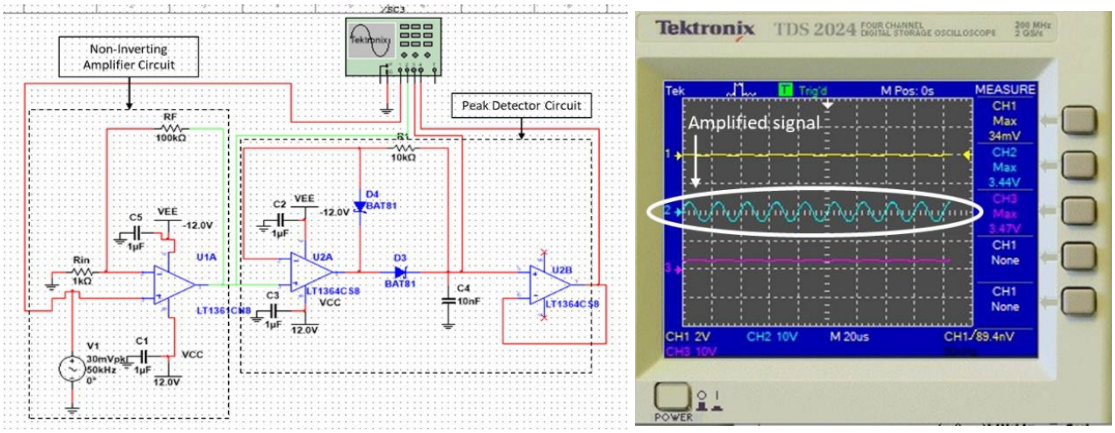

Figure 6. First schematic diagram and its simulation results of signal conditioning circuit

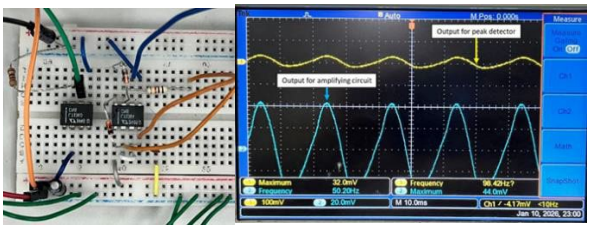

Figure 7. Real circuit construction and result

Thus, a second version of a non-inverting amplifying circuit simulation on Multisim was developed to at least amplify the output from the sensor's receiver channel. The op-amp IC was also changed from LT1361 to LT1360 because the LT1361 is a dual package that contains two op-amps, and the circuit design required only a single amplifier, so the LT1360 was chosen to match the circuit, considering that it is the single version with the same performance characteristics as in Figure 8(a). The circuit designed in the Multisim simulation was implemented on the breadboard, with the resulting data presented in Figure 8 (b).

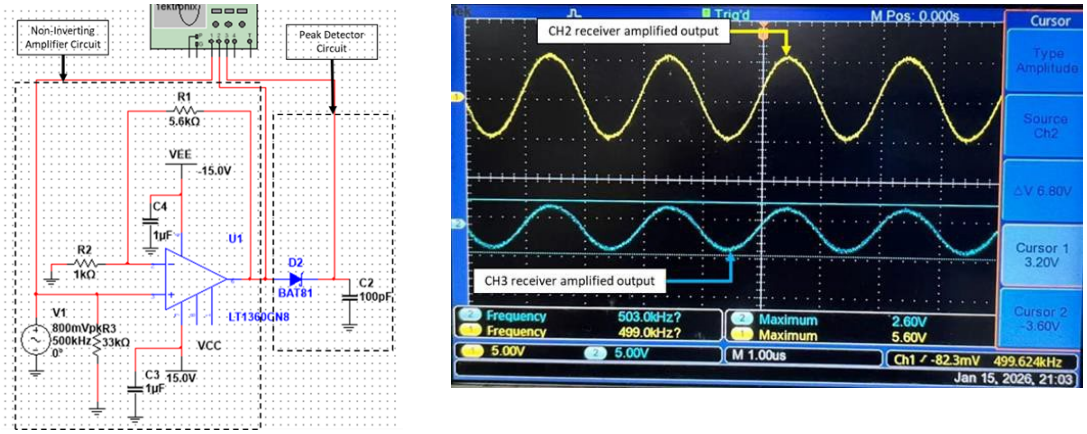

(a) (b)

Figure 8. (a) Second version of the circuit of signal conditioning; (b) Example output of the second version of the non-inverting circuit for channel 2 and channel 3

The output of the real construction of the second version of the circuit was successfully amplified, and readings of Channel 2 and Channel 3 were captured, achieving the gain, except for the peak detector part. Later, the sensor performance is evaluated based on the voltage amplitudes of the amplified signals collected during each test condition. Then, the overall measurement cycle will be made until each channel has been used as the excitation source, and there will be 12 data points for all 4 channels of the receivers (refer to Table 1). The 'x' mark will be recorded with the amplitude

values. The recorded results for this project are focused on when channel 1 was set as the transmitter, and the other three channels as the receivers.

Table 1. Measurement data table for 4 channels of ECT sensor

Tx/Rx	Rx1	Rx2	Rx3	Rx4
Tx1		x	x	x
Tx2	x		x	x
Tx3	x	x		x
Tx4	x	x	x	

2.4. GUI for Data Analysis

A MATLAB App Designer GUI was developed to simplify data analysis. Graphs were plotted using the 'UIAxes' component, images displayed with 'Image', and experimental conditions selected via a 'DropDown' menu. A "Plot" button was added to execute graph plotting for each condition. As the components have been set up, the coding has to be executed. Whereas the most important part is when the plot button was clicked, MATLAB would load the data from a CSV file that has the experiment results to be displayed and plotted in the graph, and an image will load according to its respective selected condition simultaneously. There are 7 conditions, but the 8th one is the comparison of all conditions, where the app loops through all seven CSV files and extracts one transmitter row from each and overlays them on the same graph plot with labels. Then, Figure 9 shows the MATLAB offline GUI interface for better and smooth analysis for each condition.

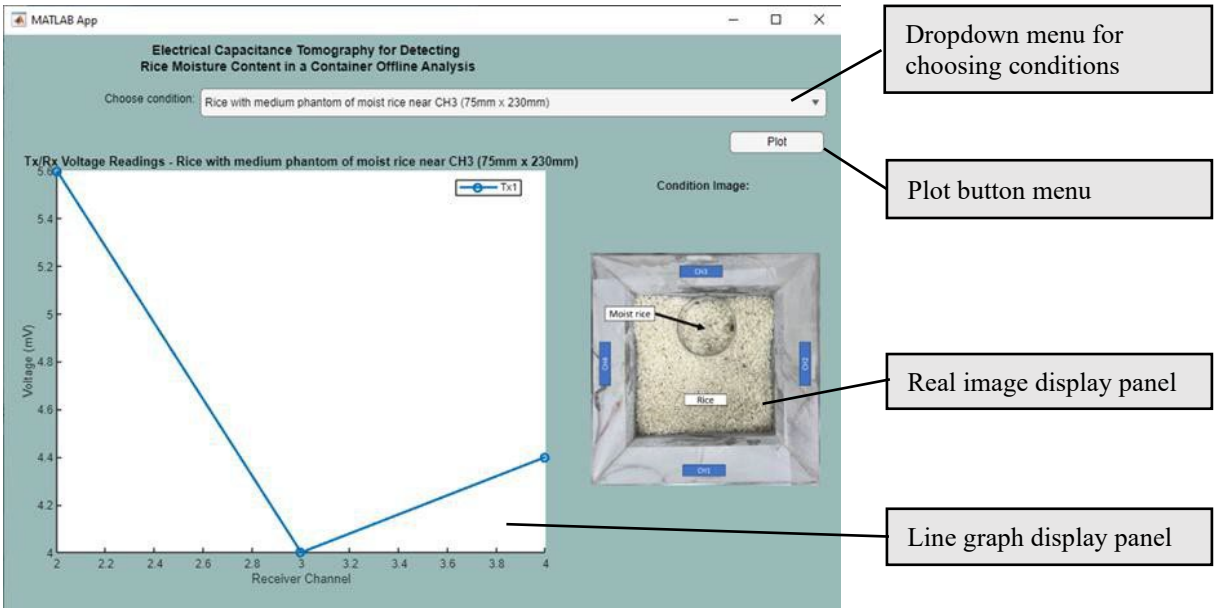

Figure 9. MATLAB Offline GUI Interface

3. Results and Discussion

The purpose of this experiment is to see whether there are any differences in the output taken from the oscilloscope under different conditions of when the rice in the container had moisture obstacles, with and without moisture, tested with several conditions like differences in size, position, and number of phantoms. The readings are recorded for comparison during the data analysis. The GUI was used for easy data analysis in this part. The material of the obstacle used was moist rice filled in phantoms with a 75mm diameter and 135mm height for the small sized phantom, 75mm diameter and 230mm height for the medium sized phantom, and 110mm diameter and 240mm height for the large sized phantom, placed at several positions in the rice container. Figure 10 shows an example of the rice in the container along with the other condition that varies.

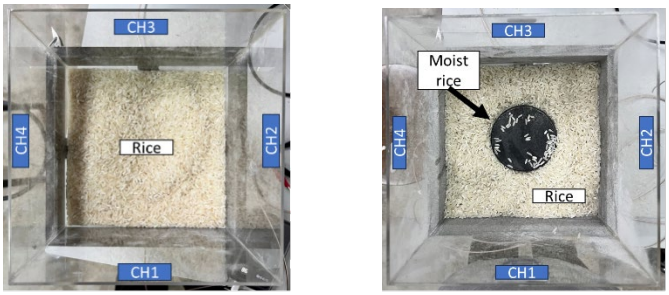

(a) (b)

Figure 10. Example of the rice in container along with the other condition that varies.

Figure 11 shows the comparison of voltage readings between rice-only and other conditions, which are the rice in the container put together with phantoms with different sizes at the same position, which is the center. The comparison between rice-only and rice with phantoms of different sizes shows a difference in voltage responses between the receivers. For the rice only condition, the readings were low. When small, medium, and large phantoms were included, the voltage increased significantly. The small and medium phantoms have a similar average output, which is 5.73V, while the large phantom has an average output reading of 5.25V. These readings show that phantom size affects the dielectric response differently.

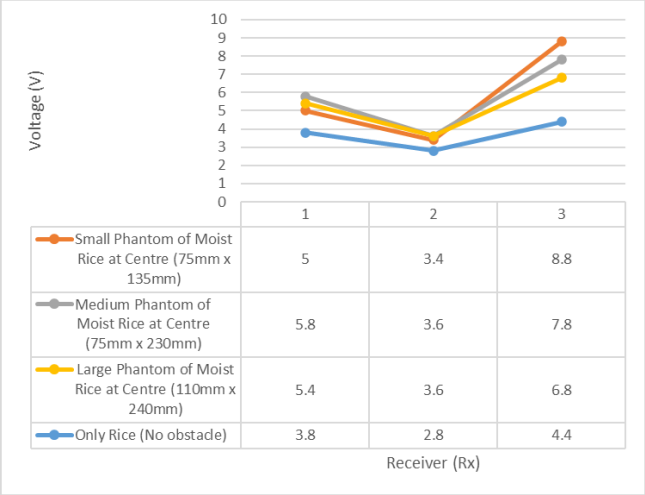

	1	2	3
Small Phantom of Moist Rice at Centre (75mm x 135mm)	5	3.4	8.8
Medium Phantom of Moist Rice at Centre (75mm x 230mm)	5.8	3.6	7.8
Large Phantom of Moist Rice at Centre (110mm x 240mm)	5.4	3.6	6.8
Only Rice (No obstacle)	3.8	2.8	4.4

Figure 11. Comparison of voltage readings between the rice-only and various phantom sizes positioned at the same location

Besides, Figure 12 shows that the results indicate that the "Only Rice (No obstacle)" condition consistently produces the lowest voltage readings across all three receivers compared to the conditions involving moist rice phantoms. The "Medium Phantom of Moist Rice at Bottom Left" and "Centre" positions show a considerable increase in voltage at Receiver 3 with peak values of 8.8V and 7.8V respectively. Receivers 1 and 2 display generally steady or slightly diminishing trends, whereas Receiver 3 has the highest sensitivity to the spatial positioning of the moist rice phantoms.

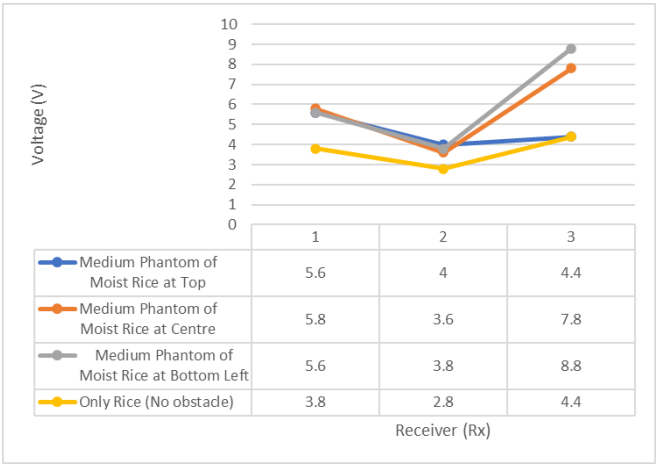

	1	2	3
Medium Phantom of Moist Rice at Top	5.6	4	4.4
Medium Phantom of Moist Rice at Centre	5.8	3.6	7.8
Medium Phantom of Moist Rice at Bottom Left	5.6	3.8	8.8
Only Rice (No obstacle)	3.8	2.8	4.4

Figure 12. Comparison of voltage readings between rice-only and other conditions with same size of phantom at different positions

It can also be shown in Figure 13, that the experimental findings of both tests show that the voltage readings are always higher when the rice phantoms are moist than when there is no impediment (just rice). Receiver 3 is the most sensitive to the spatial changes with a maximum voltage of 8.8 V for one medium phantom and 7 V for numerous small phantoms. Although Receivers 1 and 2 have more reliable answers, the aggregate results reveal that the system correctly distinguishes different phantom topologies and positions using voltage variations.

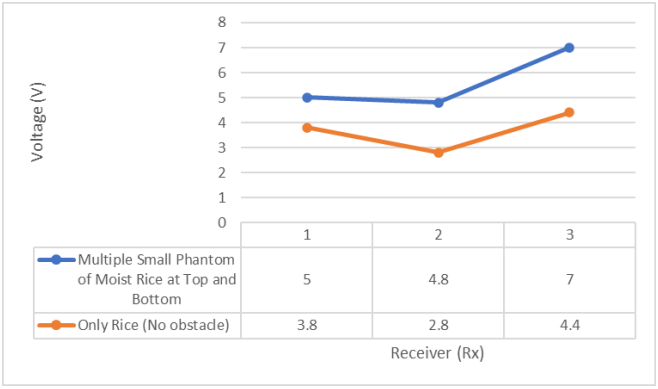

Figure 13. Comparison of voltage readings between rice-only and multiple phantoms

4. Conclusions

ECT was proved to be a non-invasive way to measure the moisture level of rice in a container and prevent the natural process of the rice tested. The results show that the presence of water impacts the voltage responses among the receivers but the voltage responses are lower in the rice-only condition. The phantom size also caused significant changes in voltage showing the effect of spatial position on the sensitivity of the device. The system was capable of differentiating between complex compositions as adding more than one phantom consistently provided greater readings than the baseline rice-only. The work shows the potential of ECT as a non-invasive real-time tool to monitor crop moisture. Future work includes improvement of circuit performance, including tomogram reconstruction for spatial imaging and scaling of the system for industrial grain storage applications.

Acknowledgement

The author gratefully acknowledges Universiti Malaysia Pahang Al-Sultan Abdullah for the financial support and access to laboratory facilities that made this research possible.

Funding

The authors would like to thank the Universiti Malaysia Pahang Al-Sultan Abdullah for providing the necessary resources and equipment for this project. This study was not supported by any grants from funding bodies in the public, private, or not-for-profit sectors.

Declaration of Competing Interest

The authors declare no conflicts of interest.

CRediT Authorship Contribution Statement

M.M. Rahman (Conceptualization; Formal analysis; Visualisation; Supervision)
Farrina Izzati Faizal Nor (Methodology; Formal analysis; Investigation; Software; Visualisation)
Mohd Mawardi Saari (Methodology; Visualisation; Data curation)
Nurul A'in Nadzri (Data curation; Project administration)
Ruzairi Abdul Rahim (Resources; Writing- review & editing)
Sia Yee Yu (Supervision; Validation)
Yasmin Abdul Wahab (Supervision; Conceptualisation; Validation)

Ethical Declaration

This research did not involve any human participants, animals, or sensitive personal data. Therefore, ethical approval was not required. All data used in this study were obtained from publicly available sources and used in accordance with relevant guidelines and regulations.

Generative Artificial Intelligence Declarations

Artificial intelligence tools were used to assist in drafting sections of the manuscript and summarizing literature. The authors reviewed and verified all AI-generated content to ensure accuracy and originality. Final interpretations and conclusions are the responsibility of the authors.

REFERENCES

[1] P. Klomklao, S. Kuntinugunetanon, and W. Wongkokua, "Moisture content measurement in paddy," in Journal of Physics: Conference Series, Institute of Physics Publishing, Oct. 2017. doi: 10.1088/1742-6596/901/1/012068.
[2] A. Aziz, G. Mugwaneza, J. C. Nshimiyimana, A. Dhiya Rachmah, and T. Park, "Moisture sensing technologies for grain storage: From single sensors to intelligent multisensory system," Precision Agriculture Science and Technology, vol. 7, no. 4, pp. 421–435, 2025, doi: 10.22765/pastj.20250028.
[3] E. Kiaitsi et al., "Real-time CO2 monitoring for early detection of grain spoilage and mycotoxin contamination," J. Sci. Food Agric., vol. 105, no. 15, pp. 8985–8993, Dec. 2025, doi: 10.1002/jsfa.70151.
[4] H. Kong, J. Wang, G. Lin, J. Chen, and Z. Xie, "Analysis of Nutritional Content in Rice Seeds Based on Near-Infrared Spectroscopy," Photonics, vol. 12, no. 5, May 2025, doi: 10.3390/photonics12050481.
[5] P. Phanomupatum, R. Phromloungsri, D. Wongpatsa, T. Pongthavornkamol, P. Saeng-On, and S. Sonasang, "Efficient and Non-Invasive Rice Moisture Quantification Using Coupled Lines Microwave Sensor Design," in 8th International Conference on Information Technology 2024, InCIT 2024, Institute of Electrical and Electronics Engineers Inc., 2024, pp. 473–478. doi: 10.1109/InCIT63192.2024.10810531.
[6] J. Liu, S. Qiu, and Z. Wei, "Real-Time Measurement of Moisture Content of Paddy Rice Based on Microstrip Microwave Sensor Assisted by Machine Learning Strategies," Chemosensors, vol. 10, no. 10, Oct. 2022, doi: 10.3390/chemosensors10100376.
[7] H. Mousazadeh, N. Tarabi, and J. Taghizadeh-Tameh, "A fusion algorithm for mass flow rate measurement based on neural network and electrical capacitance tomography," Measurement (Lond)., vol. 231, no. August 2023, p. 114573, 2024, doi: 10.1016/j.measurement.2024.114573.
[8] Z. Gut, A. Lisowski, J. Klonowski, and A. Świętochowski, "Assessing the capability of electrical capacitance tomography for monitoring chopped maize mass flow rates in field forage harvesters," Sci. Rep., vol. 15, no. 1, Dec. 2025, doi: 10.1038/s41598-025-97427-z.
[9] R. Pérez-Campos, J. Fayos-Fernández, and J. Monzó-Cabrera, "Permittivity measurements for roasted ground coffee versus temperature, bulk density, and moisture content," Journal of Microwave Power and Electromagnetic Energy, vol. 57, no. 2, pp. 102–116, 2023, doi: 10.1080/08327823.2023.2206666.
[10] L. Yu, M. Zhang, D. Yang, L. Loescher, and M. Soleimani, "Grain Moisture Sensing Using Electrical Capacitance Tomography," IEEE Sens. J., vol. 24, no. 2, pp. 2038–2048, 2024, doi: 10.1109/JSEN.2023.3335366.
[11] E. Herrera, O. Oms, and E. Remacha, "Porosity and Permeability Estimations from X-Ray Tomography Images and Data Using a Deep Learning Approach," Applied Sciences (Switzerland), vol. 16, no. 3, Feb. 2026, doi: 10.3390/app16031613.
[12] G. Kłosowski, A. Hoła, T. Rymarczyk, M. Mazurek, K. Niderla, and M. Rzemieniak, "Using Machine Learning in Electrical Tomography for Building Energy Efficiency through Moisture Detection," Energies (Basel)., vol. 16, no. 4, Feb. 2023, doi: 10.3390/en16041818.
[13] H. S. Hamzah, A. E. C. Man, Y. A. Wahab, N. A. Talip, and M. M. Saari, "Development of Image Reconstruction for Detecting Static Oil-Gas Regimes using Invasive Electrical Capacitance Tomography in Steel Application - An Initial Study," J. Teknol., vol. 86, no. 3, pp. 135–143, May 2024, doi: 10.11113/jurnalteknologi.v86.20994.
[14] A. E. C. Man et al., "Revealing the Unseen: A Brief Review of Invasive and Non-Invasive Process Tomography in Industry," J. Teknol., vol. 87, no. 4, pp. 793–807, Jul. 2025, doi: 10.11113/jurnalteknologi.v87.23257.
[15] R. C. Youngquist, J. M. Storey, M. A. Nurge, and C. J. Biagi, "A derivation of the electrical capacitance tomography sensitivity matrix," Meas. Sci. Technol., vol. 34, no. 2, Feb. 2023, doi: 10.1088/1361-6501/aca0b1.
[16] A. Eazriena Che Man et al., "Simulation of Frequency Selection For Invasive Approach of Electrical Capacitance Tomography For Conducting Pipe Application Using Oil-Gas Regimes," in 2022 Engineering Technology International Conference, ETIC 2022, 2022, pp. 63–68. doi: 10.1049/icp.2022.2571.
[17] Q. Zhao, S. Liu, and W. Chen, "A Novel Computational Imaging Algorithm for Electrical Capacitance Tomography," Applied Science-Bassel, vol. 14, no. 2, Jan. 2024, doi: 10.3390/app14020587.
[18] Z. Guo and J. Ren, "Three-Dimensional Electrical Capacitance Tomography Based on a Novel Planar Array Capacitance Sensor," Electron. Lett., vol. 61, no. 1, Jul. 2025, doi: 10.1049/ell2.70340.
[19] Y. Yang, G. Liu, and J. Liu, "A Permittivity Imaging Method: Electrical Capacitance Tomography Based on Electromagnetic Momentum," IEEE Trans. Instrum. Meas., vol. 73, 2024, doi: 10.1109/TIM.2024.3370790.
[20] J. Lei and Q. Liu, "Data and measurement mechanism integrated imaging method for electrical capacitance tomography," Appl. Soft Comput., vol. 155, Apr. 2024, doi: 10.1016/j.asoc.2024.111436.